CONTROL ID: 695594 **TITLE:** Exploring Alternative Parameterizations for Snowfall with Validation from Satellite and Terrestrial Radars **PRESENTATION TYPE:** Assigned by Committee **SECTION/FOCUS GROUP:** Atmospheric Sciences (A) **SESSION:** Development and Application of Simulators for Aerosol-Cloud-Precipitation Observation from Space (A12) **AUTHORS (FIRST NAME, LAST NAME):** Andrew Molthan[1], Walter Arthur Petersen[1], Jonathan Case[2], Scott Dembek[3] **INSTITUTIONS (ALL):** 1. NASA Marshall Space Flight Center, Huntsville, AL, USA.
2. ENSCO Inc./Short-term Prediction Research and Transition (SPoRT) Center, Huntsville, AL, Huntsville, AL, USA.
3. Universities Space Research Association/SPoRT Center, Huntsville, AL, USA.
Title of Team:

ABSTRACT BODY: Increases in computational resources have allowed operational forecast centers to pursue experimental, high resolution simulations that resolve the microphysical characteristics of clouds and precipitation. These experiments are motivated by a desire to improve the representation of weather and climate, but will also benefit current and future satellite campaigns, which often use forecast model output to guide the retrieval process. The combination of reliable cloud microphysics and radar reflectivity may constrain radiative transfer models used in satellite simulators during future missions, including EarthCARE and the NASA Global Precipitation Measurement.

Aircraft, surface and radar data from the Canadian CloudSat/CALIPSO Validation Project are used to check the validity of size distribution and density characteristics for snowfall simulated by the NASA Goddard six-class, single-moment bulk water microphysics scheme, currently available within the Weather Research and Forecast (WRF) Model. Widespread snowfall developed across the region on January 22, 2007, forced by the passing of a midlatitude cyclone, and was observed by the dual-polarimetric, C-band radar King City, Ontario, as well as the NASA 94 GHz CloudSat Cloud Profiling Radar. Combined, these data sets provide key metrics for validating model output: estimates of size distribution parameters fit to the inverse-exponential equations prescribed within the model, bulk density and crystal habit characteristics sampled by the aircraft, and representation of size characteristics as inferred by the radar reflectivity at C- and W-band.

Specified constants for distribution intercept and density differ significantly from observations throughout much of the cloud depth. Alternate parameterizations are explored, using column-integrated values of vapor excess to avoid problems encountered with temperature-based parameterizations in an environment where inversions and isothermal layers are present. Simulation of CloudSat reflectivity is performed by adopting the discrete-dipole parameterizations and databases provided in literature, and demonstrate an improved capability in simulating radar reflectivity at W-band versus Mie scattering assumptions.
http://weather.msfc.nasa.gov/sport

Exploring Alternative Parameterizations for Snowfall With Validation from Satellite and Terrestrial Radars

[1]Andrew L. Molthan, [1]Walter A. Petersen, [2]Jonathan L. Case, and [3]Scott R. Dembek

[1]NASA Marshall Space Flight Center, Huntsville, AL,

[2]ENSCO, Inc./Short-term Prediction Research and Transition (SPoRT) Center, Huntsville, AL, and [3]NASA SPoRT, Huntsville, AL

Corresponding Author: andrew.molthan@nasa.gov

http://weather.msfc.nasa.gov/sport

A21D-0273

Introduction

➢Operational weather forecast models continue their transition to higher resolution and use of bulk water schemes in the prediction of precipitaiton.
➢Each includes assumptions related to snow crystal size distributions.
➢Here, the NASA Goddard scheme is compared to observations from the Canadian CloudSat/CALIPSO Validation Project (C3VP) for the 22 January 2007 snowfall event, including C-band and CloudSat radar reflectivity.
➢**Fixed values of the snow crystal (aggregate) size distribution intercept and density are replaced with a parameterization for the distribution slope parameter and density.**

Model Simulation and Use of C3VP Data

➢The WRF model and NASA Goddard microphysics scheme is used to simulate snowfall from the 22 January 2007 synoptic scale event [Figure 1], based upon previous success by Shi et al. (2009).
➢The forecast was initialized at 1200 UTC on 21 January 2007 and continued for 36 hours, using a triply nested grid of 9, 3 and 1 km resolution.
➢Shi et al. (2009) used the NASA Goddard shortwave and longwave radiation schemes, but the RRTM and Dudhia schemes were used here.
➢Aircraft crystal imaging probes provide estimates of snow crystal size distribution parameters based upon a moment fitting technique (Heymsfield et al. 2002), with total ice water content measured by a counterflow virtual impactor (CVI). Analysis focuses on profiles near the King City radar.
➢Effective population bulk density is calculated by distributing the total ice water content over the volume of equivalent diameter spheres.
➢Previous field campaign analyses by Ryan (2000), Heymsfield et al. (2002) and Heymsfield et al. (2004) and others suggest variability in snow crystal size distributions and density, rather than the use of fixed constants.
➢**The λ(T) and $\rho(\lambda)$ relationships of Ryan (2000) and Heymsfield et al. (2004) are implemented within an experimental forecast to examine the potential benefit of new parameterizations as alternatives to the use of fixed constants.** ***These functions replace the constants applied in the NASA Goddard scheme.***

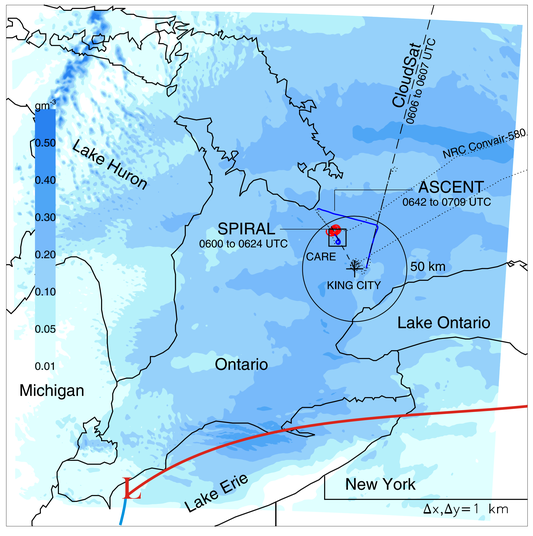

Figure 1. Snow content at the lowest altitude model vertical level, valid at 0600 UTC on 22, January 2007, based upon initial and boundary conditions from the NCEP GFS model and the NASA Goddard single-moment microphysics scheme. Location of C3VP campaign assets are indicated: the Canadian Center for Atmospheric Research Experiments (CARE), the King City radar, the CloudSat flight track, and the flight track of the NRC Convair-580 aircraft. Aircraft data segments used here are indicated as the descending spiral and departure ascent in the vicinity of the King City radar.

Profiles of Hydrometeor Content and Temperature

➢Simulated ice water content is comparable to CVI measurements [Figure 2a].
➢The water vapor profile departs from observations above 3 km due to a temperature threshold in the saturation adjustment scheme used here [Figure 2b].
➢The model temperature profile is nearly isothermal in the lowest 3 km and includes a slight warm bias throughout the entire vertical column [Figure 2c].

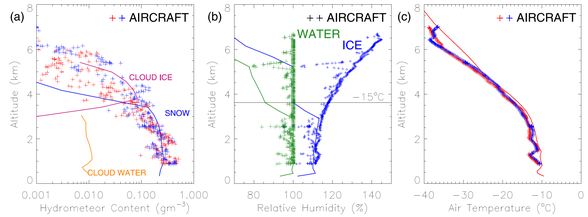

Figure 2. Mean vertical profiles of model output variables obtained from a 9 km by 9 km region centered on the King City radar, compared with C3VP aircraft observations from the spiral (red) and ascent (blue) profiles referenced in Figure 1. (a) Hydrometeor content versus measurement from the counterflow virtual impactor (CVI). (b) Saturation with respect to water or ice. (c) Air temperature from the model versus aircraft data.

Profiles of Distribution Parameters and Density

➢The fixed distribution intercept is incapable of representing vertical variability in nature, where the intercept increases with altitude [Figure 3a].
➢The use of a fixed snow bulk density fails to represent the decrease in density (aggregation) that continues from cloud top toward cloud base [Figure 3b].
➢The combination of a fixed intercept and density produces a slope that is nearly invariant in the lowest 3 km, based on conservation of ice mass [Figure 3c].

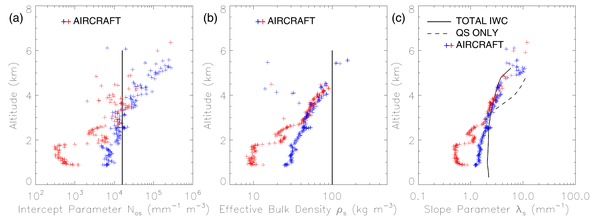

Figure 3. Mean vertical profiles of snow crystal size distrbution parameters and density, compared to model output near the King City radar. Vertical lines represent the fixed values used within the NASA Goddard scheme. (a) Distribution intercept parameter. (b) Snow bulk density. (c) Distribution slope parameter.

Parameterizations Developed from C3VP Data

➢Parameterized the distribution slope with temperature following Ryan (2000) [Figure 4a] and snow bulk density with slope following Heymsfield et al. (2004), but fit each to measurements derived from C3VP aircraft data [Figure 4a].
➢Modified the terminal velocity-diameter relationship using surface data provided by GyuWon Lee, available from the HVSD available at the CARE site [Figure 4c].

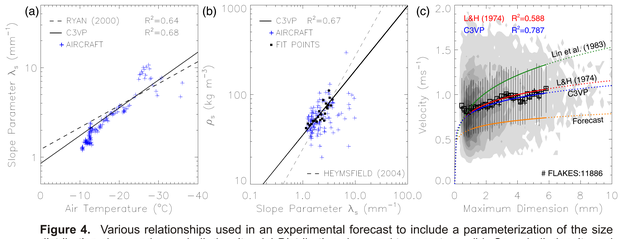

Figure 4. Various relationships used in an experimental forecast to include a parameterization of the size distribution slope and snow bulk density. (a) Distribution slope and temperature. (b) Snow bulk density and distribution slope. (c) Diameter and terminal velocity relationships from C3VP and other analyses.

Evaluation Using C3VP Aircraft Data

➢Predicted values of the slope parameter are less than those in the control forecast, but still greater than many values obtained from aircraft data [Figure 5a].
➢Overestimation of the distribution slope contributes to errors in density, but the modification is an improvement upon the previous constant value [Figure 5b].
➢The vertical profile of the distribution intercept is improved [Figure 5c].

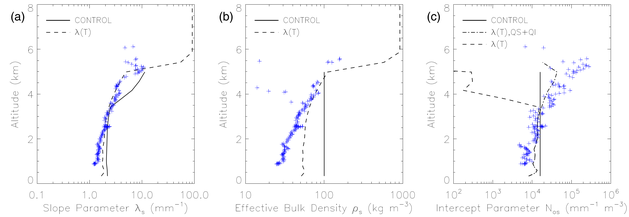

Figure 5. As in Figure 3 but based upon results from a modified NASA Goddard scheme that incorporates the parameterizations of the distribution slope, snow bulk density and fall speeds shown in Figure 4.

Comparisons to the King City Radar

➢Contoured frequency with altitude diagrams (CFADs, Yuter and Houze 1995) are used to compare observed radar reflectivity to values simulated from WRF model profiles, using intervals of 2 dB on the native model vertical levels.
➢The control forecast provides a reasonable representation, but the good fit above 3 km is only obtained when the mondisperse cloud ice category is represented by the characteristics of the simulated snow aggregates [Figure 6a].
➢Little change is noted in the CFAD from the experimental forecast in the lowest 3 km where snow is predicted, but the new parameterization reveals some issues with complex temperature profiles [Figure 6b].
➢When the model generates an isothermal or weakly inverted profile, the median profile of reflectivity oscillates, despite the asymptotic shape in nature [Figure 6c].

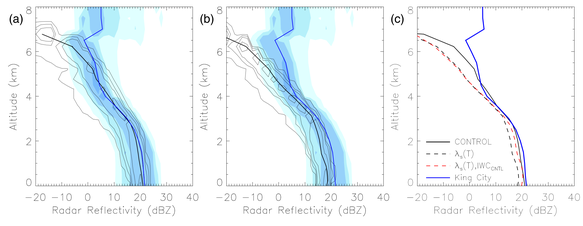

Figure 6. Comparison of CFADs from the King City radar (color filled) and the (a) control NASA Goddard scheme forecast, (b) a forecast using the aforementioned, new parameterizations and (c) a comparison of the median profiles from each simulation against King City data. Contours are at intervals of 1, 5, 10, 25 and 50% for each CFAD, with median profiles given as a single line.

Simulation of CloudSat Reflectivity

➢The forecast model assumes a spherical shape for snow crystals (low density) and for cloud ice (pure ice density), which translates naturally to use of Mie spheres.
➢Although the cloud ice category is monodisperse in the simulation, aircraft observations support a power-law size distribution similar to Heymsfield and Platt (1984). Their size distribution parameterization is utilized for model predictions of cloud ice to provide a better representation of size distributions observed by the aircraft, and presumably, the CloudSat radar.
➢Reflectivity from snow crystals is obtained from Mie spheres with densities and size distributions predicted by the NASA Goddard or experimental forecasts.
➢As an alternative, reflectivity is simulated by combining the model prediction of total ice water content with radar backscatter calculated from Ishimoto (2008) parameterizations for low density fractal aggregates.
➢Although pristine crystals were observed near cloud top, an assumption of aggregates throughout the column provides for evaluation of the snow category based upon the characteristics of the control or experimental forecast.

CloudSat Reflectivity from Mie Spheres

➢CloudSat reflectivity steadily increases from cloud top to cloud base [Figure 7a].
➢Overestimation of reflectivity above 3 km is likely due to differences in ice water content between the simulation and clouds sampled by Heymsfield and Platt (1984). Despite an overestimate, the lapse rate is reasonable [Figures 7a and 7b].
➢**Mie spheres produce a reflectivity mode below 3 km that fails to represent the observed lapse rate, due to Mie resonance for spheres larger than 0.9 mm.**
➢Despite improving upon the representation of snow characteristics in the experimental forecast [Figure 5], the increased mean size of simulated aggregates contributes to a decrease in the median reflectivity below 3 km [Figure 7c].

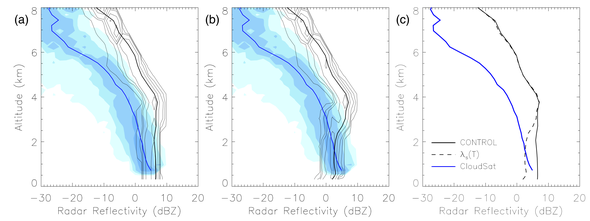

Figure 7. As in Figure 6 but for CloudSat reflectivity simulated from WRF model profiles within 25 km of the CloudSat flight track in Figure 1, based upon scattering by Mie spheres for snow and cloud ice.

CloudSat Reflectivity from Simulated Aggregates

➢Ice crystal scattering databases are valuable for the simulation of CloudSat reflectivity since natural crystals are complex in shape and poorly represented by spheres (Liu 2004, 2008 and Ishimoto 2008).
➢Low density, fractal aggregates from Ishimoto (2008) have a mass-diameter relationship comparable to the Heymsfield et al. (2004) and are used here after combining snow and cloud ice into a single measure of total ice water content.
➢Although reflectivity from CloudSat is overestimated, the lapse rate of reflectivity is better represented by assuming scattering from aggregates [Figure 8a].
➢Little change is noted in CloudSat reflectivity through use of the temperature based parameterization. The nearly isothermal nature of the model temperature profile limits variability in distribution parameters [Figure 8b].
➢**By simulating CloudSat reflectivity from Ishimoto (2008) aggregates, median reflectivity profiles [Figure 8c] do a better job of representing the observed lapse rate than Mie spheres [Figure 7c].**
➢In order to improve further, parameterizations must include functions that will overcome isothermal or inverted temperature profiles and continue the decrease in the slope parameter toward cloud base that occurs with continued aggregation.

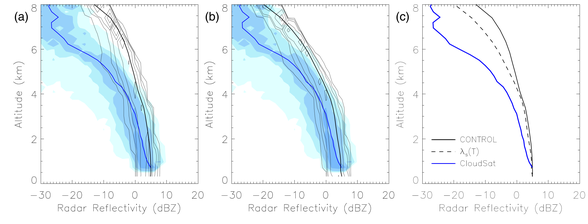

Figure 8. As in Figure 6 but for CloudSat reflectivity simulated from WRF model profiles within 25 km of the CloudSat flight track in Figure 1, based upon scattering by Ishimoto (2008) low density aggregates.

Acknowledgments

The lead author would like to thank Wei-Kuo Tao and Toshi Matsui for their guidance related to the NASA Goddard scheme and the Satellite Data Simulator Unit, Hiroshi Ishimoto for additional data required for simulating CloudSat reflectivity from aggregates, David Hudak and the C3VP data management team for access to aircraft and King City radar data, and GyuWon Lee for providing observations from the HVSD system. The lead author is supported by the NASA SPoRT Center and the Cooperative Education Program at NASA Marshall Space Flight Center. Simulations were performed using the NASA Discover computing cluster.